View metadata, citation and similar papers at core.ac.uk

brought to you by CORE

provided by Elsevier - Publisher Connector

Results in Physics 6 (2016) 420–427

Contents lists available at ScienceDirect

Results in Physics

journal homepage: www.journals.elsevier.com/results-in-physics

Electrical conductivity and dielectric studies of MnO_2 doped V_2O_5

Tan Foo Khoon [a,*], Jumiah Hassan [a,b], Zaidan Abd. Wahab [b], Raba'ah Syahidah Azis [a,b]

[a] Institute of Advanced Technology (ITMA), Universiti Putra Malaysia, 43400 Serdang, Selangor, Malaysia
[b] Department of Physics, Faculty of Science, Universiti Putra Malaysia, 43400 Serdang, Selangor, Malaysia

ARTICLE INFO

Article history:
Received 28 June 2016
Accepted 25 July 2016
Available online 30 July 2016

Keywords:
Dielectric properties
Electrical conductivity
Mixed oxides
Manganese oxide
Vanadium oxide

ABSTRACT

The investigation on electrical conductivity and dielectric properties of mixed oxide of manganese (Mn) and vanadium (V) was carried out to study the mixed oxides response to different frequencies and different measuring temperatures. The frequency and temperature dependence of AC conductivity, dielectric constant and dielectric loss factor of mixed oxides were studied in the frequency range of 40 Hz–1 MHz and a temperature range of 30–250 °C. Since the mixed oxides are multi phase materials, hence the properties of the pure oxides are also presented in this study to discuss the multi phase behaviour of the mixed oxides. The XRD pattern shows the Mn–V oxide is multiphase and quantitative phase analysis was performed to determine the relative phases. The overall results indicate that with increasing temperature, the AC conductivity, dielectric constant, dielectric loss factor and loss tangent of the Mn–V mixed oxide increases. However, it shows an overlap in the dielectric constant at 225 °C and 250 °C due to the V_2O_5 phase in the mixed oxide. From the AC activation energy, the mixed oxides underwent conduction mechanism transition from band to hopping in the investigated frequency range. The MnV_2O_6 has relatively good resistivity, therefore the mixed oxide sintered at 550 °C with the highest composition of MnV_2O_6 gives the highest dielectric constant of 9845 at 1 kHz, and at 250 °C.

© 2016 The Authors. Published by Elsevier B.V. This is an open access article under the CC BY-NC-ND license (http://creativecommons.org/licenses/by-nc-nd/4.0/).

Introduction

Composite materials have a wide variety of applications in electrical devices, mobile communication systems, etc. Therefore, composite tailoring was initiated to suit the specific needs for different usage. In the past decade, there have been several researches carried out with different metal oxides due to their application in various electronic devices such as smart window [1], optical detector [2], cathode coating in high-capacity lithium batteries [3], high performance capacitor [4], thermistor [5] and others.

Transition elements have mixed valence ions, hence those compounds have unique properties and are very useful in various fields. Manganese is one of the transition elements which has a formal oxidation state from −3 to +7 such as MnO, Mn_2O_3, Mn_2O_7, etc [6]. According to pervious works, composites containing MnO_2 such as V_2O_5 [7], SnO, As_2O_3 [8], CaO [4], Fe_2O_3 [9] etc were already investigated. Also, vanadium is a transition element with variation of oxidation state ranging from +5 to +2 and it exists in many phases such as VO, VO_2, V_2O_3 or V_2O_5 [10]. V_2O_5 is widely used in thin-films device application due to its phase transition behaviour which can alter its electrical and optical properties [11].

Gouda et al. prepared mixed oxides of manganese and vanadium at different mass ratio of Mn_2O_3 and VO_2 from 90:10 to 5:95 [7]. They found that the resistivity and the thermistor constant of beta or gamma form of $Mn_2V_2O_7$ are higher compared to the well known oxides of vanadium and binary/ternary oxides of manganese, nickel and cobalt. It meant that d-block electronic configuration of V^{5+} in $Mn_2V_2O_7$ contributed to higher resistivity [12]. Therefore, the mixed oxides with higher resistivity would increase its dielectric properties. Since the dielectric properties of Mn–V oxides system has not been reported, in this paper, the electrical conductivity and dielectric properties of mixed oxides of manganese and vanadium were studied at different measuring temperatures from 30 °C to 250 °C.

Experimental details

The mixed oxides were prepared by the conventional solid state method. The starting materials vanadium (V) oxide, V_2O_5 (99.5%) and manganese (IV) oxide, MnO_2 (99.95%) with high purity were weighed according to 40 mol% of V_2O_5 and 60 mol% of $2MnO_2$.

Acetone was added to the mixture and wet ball milled for 24 h. After the drying process in the oven, the mixture was precalcined in air at 450 °C for 4 h. The precalcined powders were added with the binder Polyvinyl Alcohol (PVA) at 1wt% and pressed at 4.5

* Corresponding author.

http://dx.doi.org/10.1016/j.rinp.2016.07.011
2211-3797/© 2016 The Authors. Published by Elsevier B.V.
This is an open access article under the CC BY-NC-ND license (http://creativecommons.org/licenses/by-nc-nd/4.0/).

tonnes for 4 min to produce Mn–V oxide pellets. The pellets were finally sintered at 500 °C and 550 °C for 4 h and ready for characterization. To understand the relationship of different phases in the mixed oxide, the pure oxides MnO_2 (MO) and V_2O_5 (VO) were also prepared to compare with the binary oxides. The list of samples and their sintering temperatures are tabulated in Table 1.

The samples were examined by XRD to determine the microstructure and phase identification and the surfaces were visualized by using Field Emission Scanning Electron Microscopy (FESEM). The dielectric properties were determined using the Agilent 4294A Precision Impedance Analyzer from 30 °C to 250 °C and the sample was attached to the analyzer by sandwiching it between two copper electrodes. The dielectric constant and loss factor were calculated using: $\varepsilon_r' = Cd/\varepsilon_o A$ and $\varepsilon_r'' = Gd/\varepsilon_o \omega A$ respectively, where C is the capacitance, d is the thickness, ε_o is permittivity of free space, G is the conductance, ω is the angular velocity and A is the cross-sectional area of the sample. The AC conductivity σ_{ac} is determined from the dielectric parameter where, $\sigma_{ac} = \omega\varepsilon_o\varepsilon_r''$.

XRD were done to determine the phase identification and phase composition of the samples. Meanwhile, the composition of the phase consisted in each sample was determined by using Rietveld Refinement analysis. The surface of the samples was viewed using FESEM and the average grain size was calculated. For conductivity measurements, AC and DC conductivities were measured over the temperature range from 30 °C to 250 °C via cooling process and their activation energies were determined and discussed. For dielectric properties, the dielectric behaviour of the samples was discussed at different measuring temperatures 30 °C to 250 °C for the frequency range of 40 Hz to 1 MHz.

Results and discussion

The samples were characterized for their structural, dielectric properties and electrical conductivity.

Structural Analysis

The phase contained in the sample was identified by comparing the observed XRD patterns with Inorganic Crystal Structure Database (ICSD) pattern. Fig. 1 shows the X-ray diffraction pattern of Mn–V oxide and the compounds presented which are Manganese Divanadate, MnV_2O_6 (ICSD: 98-004-7436), Vanadium pentoxide, V_2O_5 (ICSD: 98-001-2286) and Manganese(IV) Oxide-beta, MnO_2 (ICSD: 98-001-2180) [13,14]. Practically, the single phase material is difficult to obtain because manganese and vanadium have many oxidation states [6,15] and quantitative phase analysis were performed in order to determine the percentage of the relative phase. As a result, the Rietveld Refinement analysis and the X'pert HighScore Plus software were used [16].

The XRD pattern of MVO500 and MVO550 are almost similar as shown in Fig. 1. At this stage, the Mn–V oxide is MnV_2O_6. However, the starting materials MnO_2 and V_2O_5 still remained. The increase in sintering temperature gives rise to the reaction between the starting materials to form MnV_2O_6. Therefore, the phase composition of MnO_2 and V_2O_5 decreases while MnV_2O_6 increases from

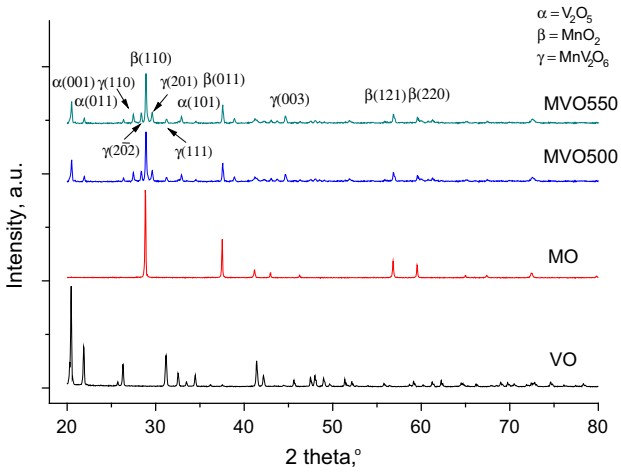

Fig. 1. XRD patterns of MO, VO, MVO500 and MVO550.

500 °C to 550 °C as shown in Table 2. Finally, we can conclude that a multiphase compounds was prepared. On the other hand, the XRD patterns of MO and VO show that the samples were successfully prepared with high purification which are MnO_2 and V_2O_5 respectively.

The morphology and grain size of the sample were determined by FESEM. 150 grains were taken randomly from the FESEM images to calculate their average grain size and this was tabulated in Table 3. Fig. 2(a) and (b) showed that the grain sizes of the starting materials are large. After mixing and wet ball milling for 24 h, the particles sizes were reduced as shown in Fig. 2(c) and (d). The grain size of MVO500 is small because the particles lack energy to react among themselves and only a small amount of diffusion between neighbouring particles occurred [17]. However, MVO550 began to attach to the neighbouring particles to grow and form a larger grain. Hence, better densification is possible at higher sintering temperature.

Electrical conductivity

AC conductivity is an electrical parameter that quantified the electrical conduction due to an applied electrical AC field in a material [18]. The AC conductivity, σ_{ac} of pure oxides and Mn–V oxide varies with different temperatures as shown in Fig. 3. The σ for the samples is found to follow the unique conductive properties of semiconductor that increases with increasing temperature. This may due to that the heat applied is able to excite more electron hops from the valence band to conduction band and increase the σ_{ac} [19]. The σ_{ac} is independent of frequency at low frequency region, but increases with frequency at the high frequency region. As temperature increases, the σ_{ac} becomes independent of frequency within 1 MHz at 250 °C. Therefore, the σ_{ac} can be described via Jonscher's universal power law [20].

$$\sigma_T(\omega) = \sigma_{dc}(0) + A\omega^s \quad (1)$$

where σ_T is the total conductivity, σ_{dc} is the DC conductivity, A is constant, ω is angular frequency and s is frequency exponent where

Table 1
List of samples at different sintering temperatures.

Sample name	Sintering Temperature, °C
MO	450
VO	600
MVO500	500
MVO550	550

Table 2
The phase composition of the compound contained in the sample of MVO500 and MVO550.

Sample	MnO_2 (%)	V_2O_5 (%)	MnV_2O_6 (%)	R-indices
MVO500	49.2	29.8	21.0	2.995
MVO550	40.4	19.5	40.1	1.907

Table 3
Average grain size of pure oxides and mixed oxides.

	MO	VO	MVO500	MVO550
Avg. grain size (μm)	2.61	2.20	0.708	0.784

$0 < s < 1$. According to Jonscher's universal power law, the frequency independence plateau region as shown in Fig. 3 is attributed to DC-like conductivity. This is probably due to the short-range pairwise hopping between the neighbouring particles. The σ_{dc} was extracted from Fig. 3 and tabulated in Table 4. As frequency increases, the change that depends on frequency is called conductivity relaxation phenomenon. This behaviour is in good agreement with the hopping relaxation model. According to this model, a charge carrier successfully hops to its neighbouring vacant site and contribute to σ_{dc} at low frequency. As frequency increases, the probability of the correlated back and forth hopping causes the relaxation of the charges carriers [21]. Fig. 3 shows that MO has higher σ_{ac} compared to VO which are 23.66 and 1.23 $m\Omega^{-1}\,m^{-1}$ at 40 Hz, 250 °C respectively. The σ_{ac} of MVO500 and MVO550 fell between MO and VO. Also, MVO550 has lower σ_{ac} than MVO500, which is possibly due to the higher phase composition of MnV_2O_6 in MVO550.

Fig. 4 shows the minimum and maximum influence of alternating applied field to σ_{ac} at 1 kHz and 1 MHz respectively for pure and mixed oxides. For pure oxides, MO has greater σ_{ac} compare to VO. They are highly temperature dependent at the low temperature region however, at a temperature beyond 175 °C, the increment of conductivity is reduced. This might be due to semiconductor-metal phase transition [15]. When the free charge carrier is in abundance as temperature increases, the resistivity caused by vibration of lattice and the collision between free charge carriers become significant [22]. Therefore, the unexpected drop of σ_{ac} at 250 °C for VO suggests that VO decreases with temperature beyond 250 °C. It can be seen that the σ_{ac} of MVO500 and MVO550 follow VO as domain of the composite. The addition of MnO_2 in the composite enhances the σ_{ac} of the mixed oxides. Therefore, the σ_{ac} of mixed oxides are higher than pure oxides at low temperature but the σ_{ac} of mixed oxides drop between MO and VO at 250 °C. The σ_{ac} decreases from 1.02 $m\Omega^{-1}\,m^{-1}$ to 0.49 $m\Omega^{-1}\,m^{-1}$ at 1 kHz, 30 °C when the mixed oxide was sintered from 500 °C to 550 °C. This may be due to the phase composition of MnV_2O_6 which has higher resistivity compared to MnO_2. Also, the decrease of MnO_2 in the composition at MVO550 resulted in the reduction of conductivity.

Activation energy for AC conduction

A century ago, activation energy, ΔE was introduced by Hood as an empirical relationship and it is temperature dependent. In this research, Arrhenius equation is used to determine the sensitivity of the current flow rate with temperature [23]. The AC activation energy, ΔE_{ac} is calculated from the Arrhenius equation [24]:

$$\sigma = \sigma_o exp\left(\frac{-\Delta E}{k_B T}\right) \tag{2}$$

where σ_o is the pre-exponential factor and K_B is Boltzmann constant. To determine the activation energy, ΔE_{ac} the behaviour of

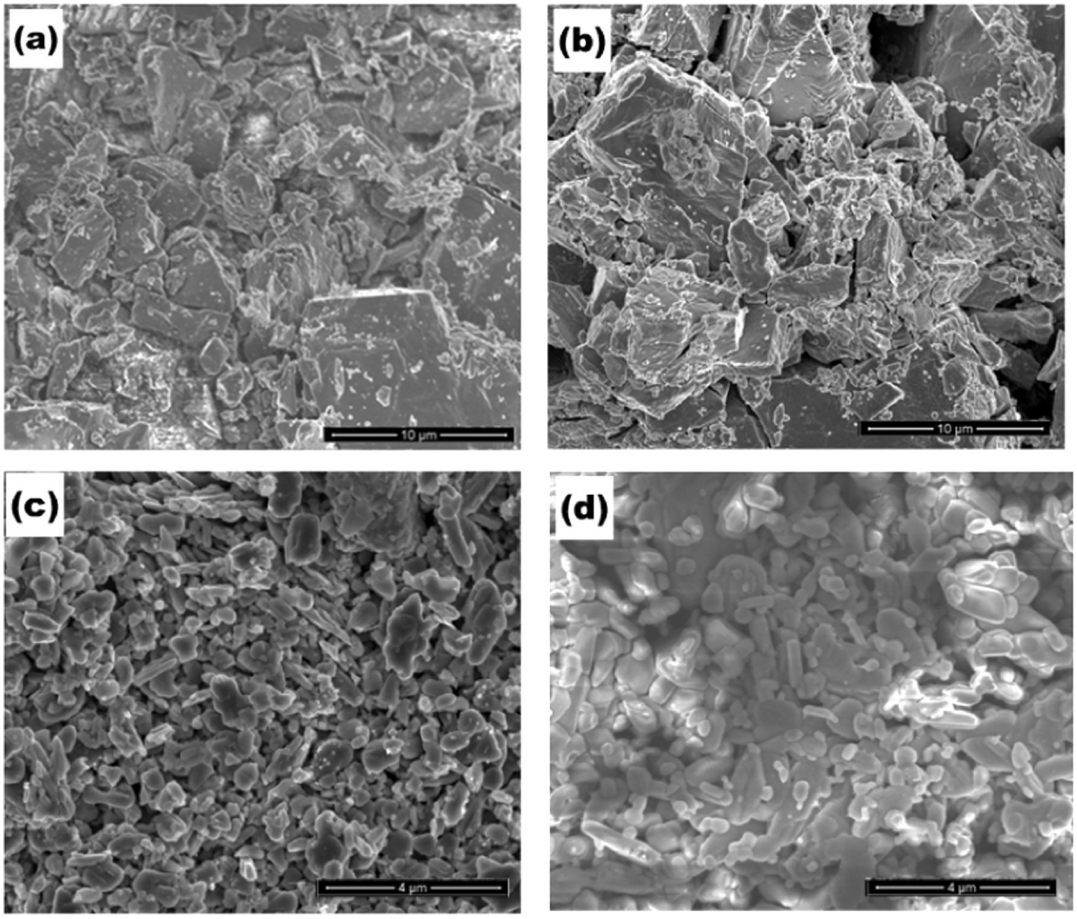

Fig. 2. FESEM images for (a) MO, (b) VO, (c) MVO500 and (d) MVO550.

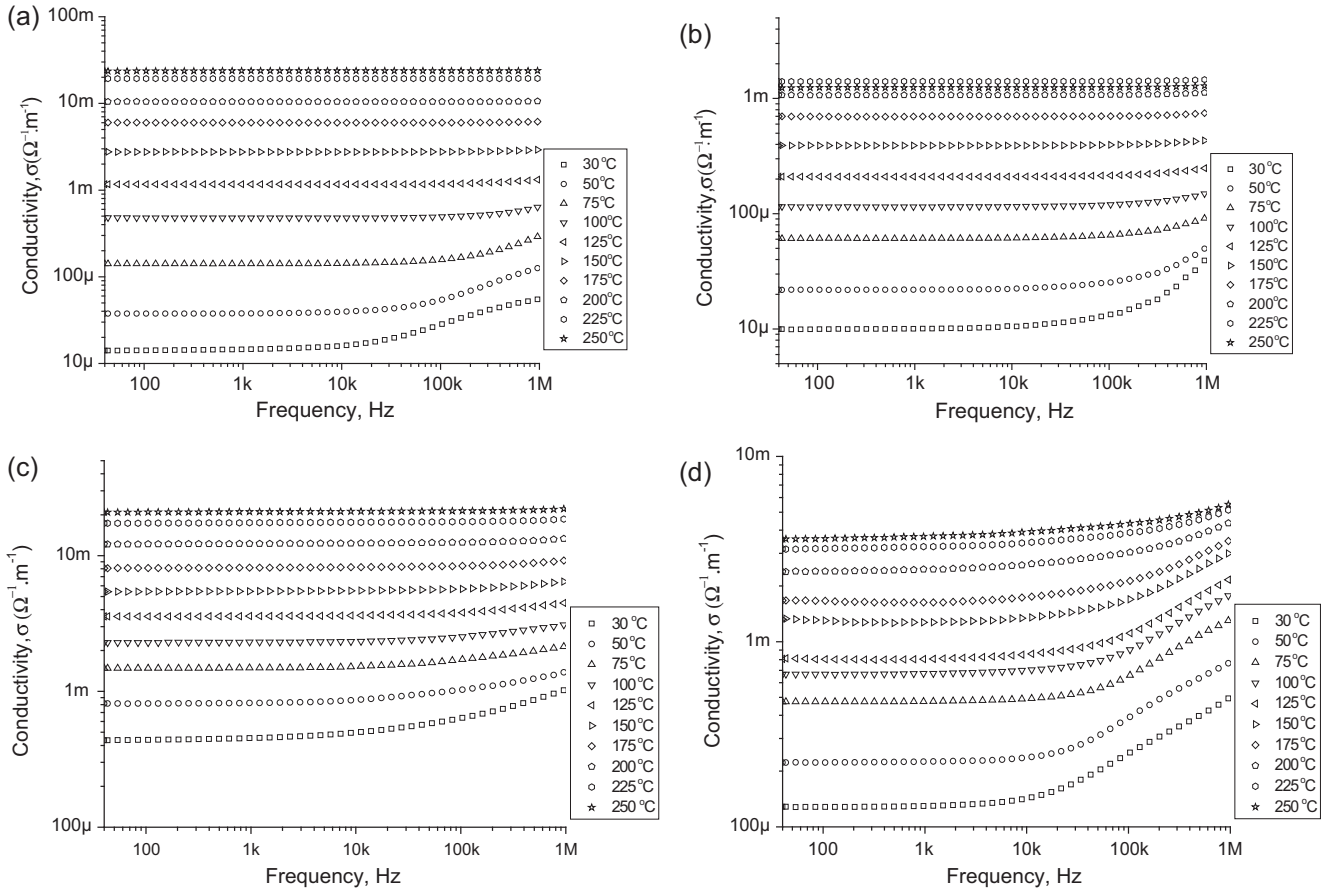

Fig. 3. Variation of AC conductivity with respect to frequency at different measuring temperatures from 30 °C to 250 °C for (a) MO, (b) VO, (c) MVO500 and (d) MVO550.

Table 4
DC-like conductivity extracted from AC conductivity spectrum at different measuring temperatures for pure and mixed oxides.

Samples	σ_{dc} (Ω^{-1} m^{-1})									
	30 °C	50 °C	75 °C	100 °C	125 °C	150 °C	175 °C	200 °C	225 °C	250 °C
MO	14.1 μ	37.6 μ	141 μ	481 μ	1.17 m	2.76 m	6.03 m	10.5 m	19.3 m	23.6 m
VO	9.94 μ	21.9 μ	60.9 μ	115 μ	210 μ	390 μ	700 μ	1.07 m	1.41 m	1.23 m
MVO500	437 μ	813 μ	1.48 m	2.29 m	3.56 m	5.42 m	8.08 m	12.2 m	17.29 m	20.83 m
MVO550	128 μ	223 μ	474 μ	667 μ	812 μ	1.33 m	1.67 m	2.38 m	3.16 m	3.58 m

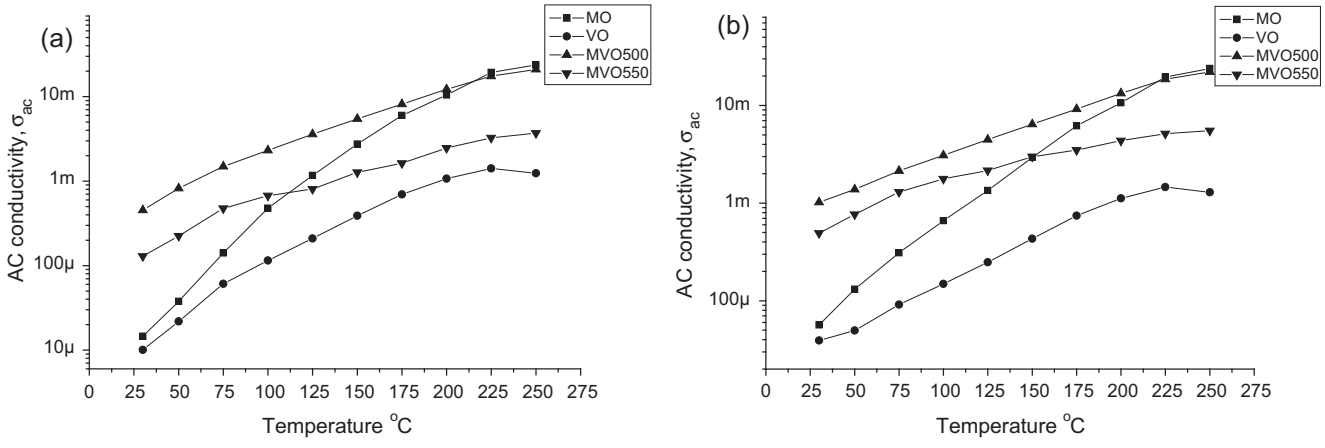

Fig. 4. Variation of AC conductivity for pure and mixed oxides from 30 °C to 250 °C at (a) 1 kHz and (b) 1 MHz.

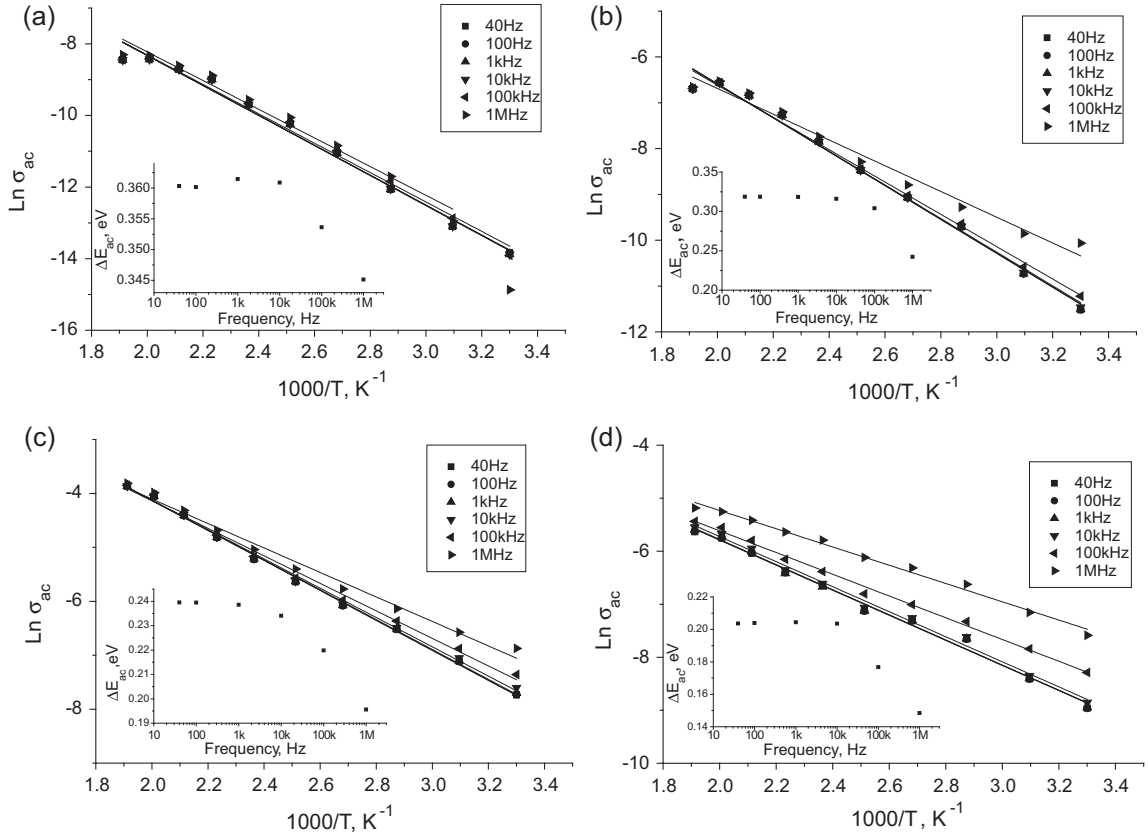

Fig. 5. Temperature dependence of $Ln\sigma_{ac}$ at different frequencies for (a) MO, (b) VO, (c) MVO500 and (d) MVO550; the inset figure represents the plot of ΔE_{ac} versus frequency.

Mn–V oxide with a linear relationship between Ln σ_{ac} and the reciprocal of temperature at different frequencies is plotted as shown in Fig. 5. The ΔE_{ac} of MO and VO remained constant at the low frequency region (40 Hz to 10 kHz) and decreases as frequency increases. This phenomenon suggests that the samples exhibit conduction transition from band conduction to hopping conduction. At low frequency, the free charge carriers need to jump from valance band to conduction band to conduct, thus they need a fixed amount of energy to overcome the energy band gap [25]. This is so-called band conduction. When the frequency increases beyond 10 kHz, the ΔE_{ac} decreases due to the frequency of the applied field improved the electronic jumps between the localized states [26]. Moreover, the frequency dependence of conductivity suggests that hopping conduction is the dominant mechanism [27].

For MVO500 and MVO550, they still have a large phase composition of MnO_2 and V_2O_5 remained (refer to Table 2). Since both MnO_2 and V_2O_5 are more conductive compared to the other phases, so the phenomenon of uniform ΔE_{ac} at the low frequency region is possible due to the band conduction [25]. The decrease of ΔE_{ac} at frequency beyond 10 kHz confirms that the conduction mechanism was changed to hopping conduction [28]. The ΔE_{ac} of MVO500 is greater than MVO550 representing the MVO500 needs more energy for the charge carriers to conduct. This indicate that MVO500 has insufficient energy to diffuse and form larger grain during the sintering process, therefore the smaller average grain size of MVO500 increases the insulating grain boundary volume and increases the ΔE_{ac} [29]. However, the σ_{ac} of MVO500 is higher than MVO550 as illustrated in Fig. 3(c) and (d). This may be due to their pre-exponential factor, σ_o as tabulated in Table 5 which is much influenced by the different phases, phase composition and electric field [30].

Dielectric properties

The frequency and temperature dependence of the dielectric constant, ε_r' for all samples are illustrated in Fig. 6. The ε_r' of all samples increases with increasing temperature and this suggests that charge carriers are at low energy state when the temperature is relatively lower. Hence, the charge carriers are difficult to move and the movement to follow the direction of the applied field is weak which results in low contribution to polarization and dielectric behaviour. With the rise in temperature, the charge carriers were excited and get enough energy to follow the change of the applied field, consequently increase the dielectric behaviour [31]. However, the VO underwent a reduction of ε_r' at 250 °C suggesting that the sample underwent semiconductor-metal phase transaction at 225 °C. For MO and VO, their ε_r' are low compared to the mixed oxides which are 10.19 and 30.61 at 1 kHz, 250 °C respectively. This may be because MnO_2 and V_2O_5 are semiconductors and they are weak in electric charge storage [32,15].

The phase composition of MVO500 and MVO550 is the main factor that can alter the ε_r'. It is clear from the graphs, ε_r' decreases with increasing frequency. This is possibly due to the electrons accumulating at the grain boundary resulting in interfacial polarization at low frequency, but as frequency increases, the decreasing ε_r' can be attributed to the transition from interfacial polarization to dipolar polarization. Interfacial polarization generally takes a longer time to form completely than other polarizations [33,34]. As temperature increases, the energy of charge carriers increases and are able to follow the direction of the applied field, thus prolonging the interfacial polarization frequency range. Therefore, we can observe the relaxation process is slowly shifting to higher frequency. Fig. 6 shows the ε_r' of MVO550 is higher than MVO500

Table 5
Activation Energy for AC conduction, ΔE_{ac} (eV) and Pre-exponential factor, σ_o (Ω^{-1} m^{-1}) of pure oxides and mixed oxides.

Samples	40 Hz		100 Hz		1 kHz		10 kHz		100 kHz		1 MHz	
	ΔE_{ac}	σ_o	ΔE_{ac}	σ_o	ΔE_{ac}	σ_o	ΔE_{ac}	σ_o	ΔE_{ac}	σ_o	ΔE_{ac}	σ_o
MO	0.360	1.04	0.360	1.03	0.361	1.07	0.360	1.05	0.354	0.90	0.345	0.81
VO	0.318	2.24	0.318	2.24	0.318	2.22	0.315	2.09	0.304	1.55	0.242	0.34
MVO500	0.239	4.17	0.239	4.18	0.238	4.11	0.234	3.69	0.219	2.63	0.195	1.55
MVO550	0.203	0.35	0.203	0.35	0.204	0.35	0.203	0.37	0.176	0.22	0.148	0.17

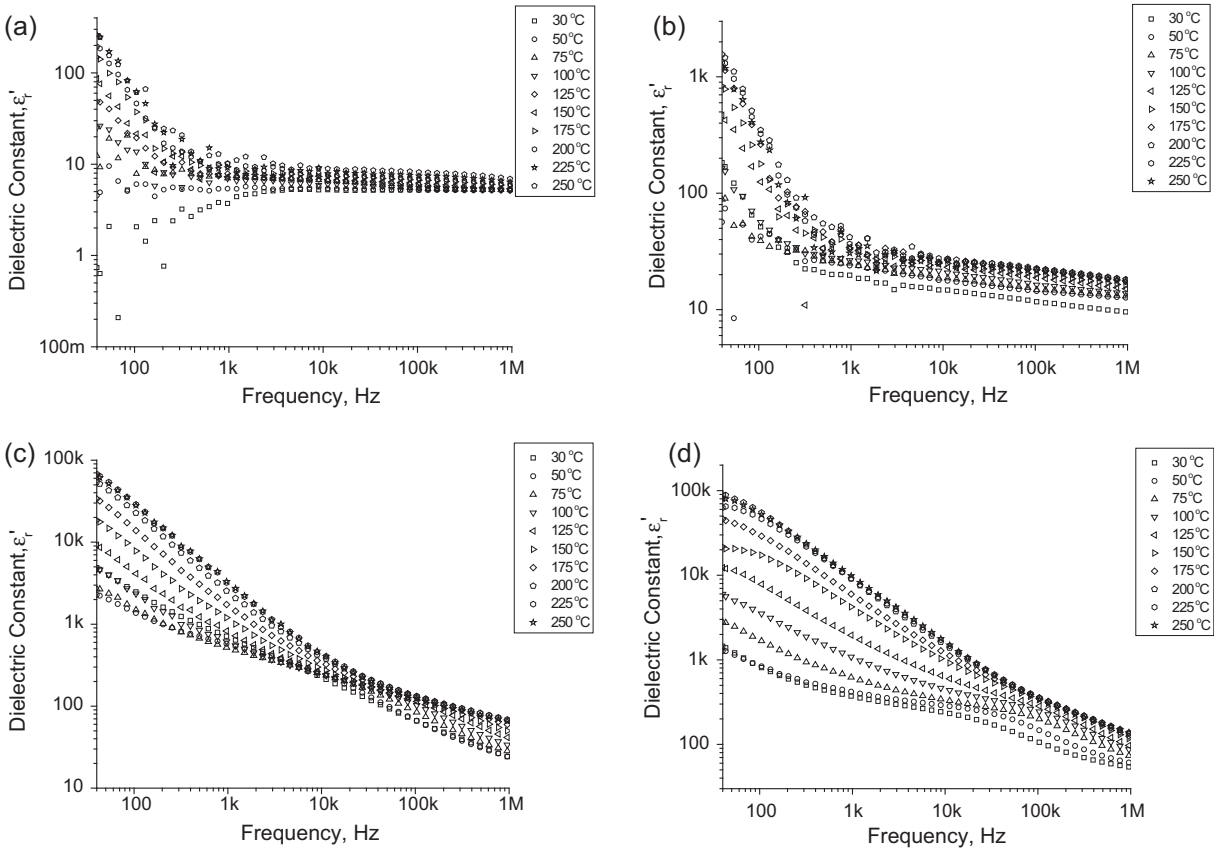

Fig. 6. Variation of the dielectric constant with respect to frequency for (a) MO, (b) VO, (c) MVO500 and (d) MVO550.

which is 9845 and 3315 at 1 kHz, 250 °C respectively. Also, ε_r' of MVO550 is less frequency dependent compared to MVO500. This indicates that the interfacial polarization frequency range increases and relaxation process is shifted to higher frequency. This might due to the MVO550 has higher phase composition of MnV_2O_6. Therefore, it can be concluded that the presence of MnV_2O_6 has higher resistivity, hence increases the ε_r' of the samples [7]. Moreover, the semiconductor-metal phase transition of V_2O_5 causes the ε_r' to overlap at 225 °C and 250 °C. The reduction of ε_r' is not as much as VO at 250 °C because of the phase composition of V_2O_5 is small.

The imaginary part of the complex permittivity is the dielectric loss factor, ε_r''. When an electric field is applied to a material, the electric energy displaces the charge carriers and energy loss transforms into heat energy known as dielectric losses. Fig. 7 shows the frequency dependence of the dielectric loss factor for pure oxides and mixed oxides at different temperatures. The dielectric loss factor is relatively high at low frequency region and decreases with the increase in frequency. At low frequency region, the high dielectric loss is caused by the migrating charge carriers and the charge carrier migration is reduced when frequency increases [19]. In addition, it is observed that the dissipated energy increases as the temperature increases and this can be attributed to the thermal effect increase of the drift velocity and hopping frequency of the charge carriers. Hence, the increase in AC conductivity results in the increase of ε_r'' [35]. From Fig. 7, we can conclude that the mixed oxides are lossy material, because the ε_r'' of the sample is very much greater than ε_r'. However, MVO550 successfully lowered the ε_r'' which is 4937 at 1 kHz, 30 °C.

Conclusion

Mn–V mixed oxides (MnV_2O_6, V_2O_5, MnO_2) was successfully prepared and they are a multi-phase material. This is confirmed by X-ray diffraction and Rietveld Refinement analysis. The AC conductivity, dielectric constant and dielectric loss factor of Mn–V oxide were studied in the frequency range of 40 Hz–1 MHz and temperature range of 30 °C to 250 °C. As temperature rises, the AC conductivity increases with increase in frequency. Therefore, AC conductivity is a thermally activated process. The activation energy of AC conduction, ΔE_{ac} is frequency independence at low

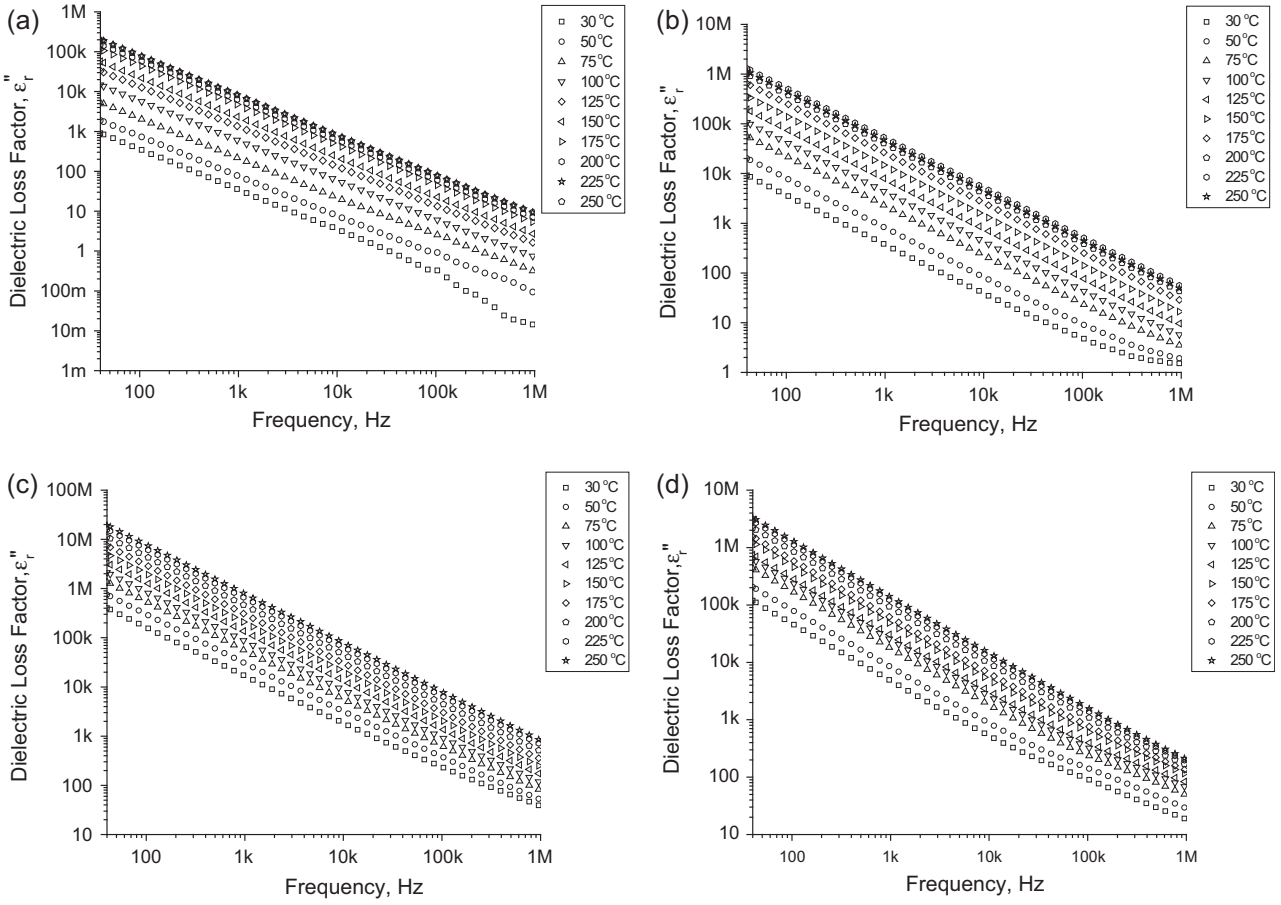

Fig. 7. Variation of the dielectric loss factor with respect to frequency for (a) MO, (b) VO, (c) MVO500 and (d) MVO550.

frequency region and decreases with increase in frequency. Hence, there is a conduction transition from band conduction to hopping conduction mechanism when frequency increases beyond 10 kHz. For dielectric properties, we can conclude that the MnV_2O_6 has relatively good resistivity, therefore the MVO550 with the highest composition of MnV_2O_6 gives the highest ε'_r of 9845 at 1 kHz, 250 °C. Also, it increases the interfacial polarization frequency range and shifts the relaxation process to higher frequency. The mixed oxides are lossy materials, so it can be used as a microwave absorber.

Acknowledgements

This work was financially supported by the Research University Grant Scheme (RUGS) Project No.: 05-02-12-2180RU, Universiti Putra Malaysia (UPM). The authors also acknowledged the Department of Physics, Faculty of Science UPM and Institute of Advanced Technology (ITMA) UPM.

References

[1] Zhangli H, Changhong C, Chaohong L, Sihai C. Tungsten-doped vanadium dioxide thin films on borosilicate glass for smart window application. J Alloy Compd 2013;564:158–61.
[2] Bin W, Jianjiun L, Hui L, Haoming H, Sihai C. Nanostructured vanadium oxide thin film with high TCR at room temperature for microbolometer. Infrared Phys Technol 2013;57:8–13.
[3] Di Blasi O, Briguglio N, Busacca C, Ferraro M, Antonucci V, Di Blasi A. Electrochemical investigation of thermically treated graphene oxides as electrode materials for vanadium redox flow battery. Appl Energy 2015;147:74–81.
[4] Yanez Vilar S, Castro-Couceiro A, Rivas-Murias B, Fondado A, Mira J, Rivas J, et al. High dielectric constant in the charge-ordered manganese oxide $CaMn_7O_{12}$. Z Anorg Allg Chem 2005;631:2192–6.
[5] Gouda GM, Nagendra C. Preparation and characterization of thin film thermistors of metal oxides of manganese and vanadium (Mn-V-O). Sens Actuators A 2013;190:181–90.
[6] Kemmitt R, Peacock, R. The Chemistry of Manganese, Technetium and Rhenium, Britain: Pergamon Texts in Inorganic Chemistry, vol. 13, 1975, p. 778–782.
[7] Gouda GM, Nagendra C. Structural and electrical properties of mixed oxides of manganese and vanadium: a new semiconductor oxide thermistor material. Sens Actuators 2009;A 155:263–71.
[8] Kayan A, Tarcan E, Kadiroglu U, Esmer K. Electrical and dielectrical properties of the MnO_2 doped with As_2O_3 and SnO. Mater Lett 2004;58:2170–4.
[9] Molenda J, Stoklosa A, Znamirowski W. Electrical properties of manganese doped ferrous oxide at high temperature. Solid State Ionics 1987;24:39–44.
[10] Walia S, Balendhran S, Nili H, Zhuiykov S, Rosengarten G, Hua Wang Q, et al. Transition metal oxides-thermoelectric properties. Prog Mater Sci 2013;58:1443–89.
[11] Ya Q, Jie C, Yuan L, Xing Y, Hua Y, Kai X. Fabrication of low phase transition temperature vanadium oxide films by direct current reactive magnetron sputtering and oxidation post-anneal method. Infrared Phys Technol 2014;67:126–30.
[12] Bordeneuve H, Guillemet-Fritsch S, Rousset A. Structure and electrical properties of single-phase cobalt manganese oxide spinels $Mn_{3-x}Co_xO_4$ sintered classically and by spark plasma sintering (SPS). Solid State Chem 2009;182:396–401.
[13] Inorganic Crystal Structural Database ICSD v2014–01, 2014.
[14] Amelo, B. X'Pert HighScore Plus, version 3.0e, The Netherlands, 2012.
[15] Xiaochun W, Fachun L, Limei L, Yongzeng L, Lianghui L, Yan Q, et al. Influence of thermal cycling on structural, optical and electrical properties of vanadium oxide thin films. Appl Surf Sci 2008;255:2840–4.
[16] Fernandez-Palacios S, Santos-Gomez L, Compana J, Porras-Vazpuez J, Cabeza A, Marrero-Lopez D, et al. Influence of the synthesis method on the structure and electrical properties of $Sr_{1-x}K_xGeO_{3-x}$. Ceram Int 2015;41:6542–51.
[17] Wang Q, Wang Q, Wan C. Effect of sintering time on the microstructure and properties of inorganic polyphosphate bioceramics. Sci Sinter 2010;42:337–43.

[18] Palgrave Macmillan Ltd. Dictionary of physics. Germany: Spektrum Akademischer Verlag; 2004.
[19] Solymar L, Walsh D. Lectures on the electrical properties of materials. Great Britain: Oxford University Press; 1979.
[20] Almond D. Mobile ion concentrations in solid electrolytes from an analysis of AC conductivity. Solid State Ionic 1983;9 & 10:277–82.
[21] Anantha P, Hariharan K. Ac Conductivity analysis and dielectric relaxation behaviour of $NaNo_3$-Al_2O_3 composites. Mater Sci Eng B 2005;121:12–9.
[22] Matula R. Electrical resistivity of copper, gold, palladium and silver. J Phys Chem Ref Data 1979;8(4):1147–298.
[23] Sudha L, Roy S, Rao KU. Evaluation of activation energy (Ea) profiles of nanostructured alumina polycarbonate composite insulation materials. Int J Mater Mech Manuf 2014;2:1.
[24] Bekheet A, Hegab N. Ac conductivity and dielectric properties of $Ge_{20}Se7_5In_5$ films. Vacuum 2009;83:391–6.
[25] Tsuda, N, Nasu, K, Yanase, A, Siratori, K. Electronic Conduction in Oxides, Germany, 1991.
[26] Yakuphanoglu F, Evin E, Okutan M. The dielectrical and alternating current conductivity properties of 40Cu+20Co+40Y2O3 ceramic. Phys B 2006;382:285–9.
[27] Yakuphanoglu F, Zaitsev D, Trusov L, Kazin P. Electrical conductivity and electrical modulus properties of 13SrO-5.5Fe_2O_3-0.5Al_2O_3-8B_2O_3 magnetic glass ceramic. J Magn Magn Mater 2007;312:43–7.
[28] Okutan M, Basaran E, Bakan HI, Yakuphanoglu F. AC conductivity and dielectric properties of Co-doped TiO_2. Phys B 2015;364:300–5.
[29] Gao W, Sammes NM. An introduction to electronic and ionic materials. Singapore: World Scientific; 1999.
[30] Kumar A, Kumar A. Dependence of activation energy and pre-exponential factor on electric field in bulk $Se_{90}Sb_{10-x}Ag_x$ glassy alloys. J Non-Cryst Solids 2014;386:51–5.
[31] Ahmed R, Moslehuddin A, Mahmood ZH, Akther Hossain A. Weak ferromagnetism and temperature dependent dielectric properties of $Zn_{0.9}Ni_{0.1}O$ diluted magnetic semiconductor. Mater Res Bull 2015;63:32–40.
[32] Fernandez J, Caballero A, Villegas M, Khatib S, Banares M, Fierro J, et al. Structure and magnetism in the Zn-Mn-O system: a candidate for room temperature ferromagnetic semiconductor. J Eur Ceram Soc 2006;26:3017–25.
[33] Hsing-I H, Chi-Shiung H, Chi-Yao T, Li-Then M. Cobalt-substitution effect on dielectric properties of CuZn ferrites. Ceram Int 2015;41:4140–4.
[34] Ranjith Kumar E, Jayaprakash R. The role of fuel concentration on particle size and dielectric properties of manganese substituted zinc ferrite nanoparticles. J Magn Magn Mater 2014;366:33–9.
[35] Ansari SA, Nisar A, Fatma B, Khan W, Chaman M. Temperature dependence anomalous dielectric relaxation in Co doped ZnO nanoparticles. Mater Res Bull 2012;47:4161–8.